JOURNAL OF GEOPHYSICAL RESEARCH, VOL. 106, NO. C10, PAGES 22,559–22,574, OCTOBER 15, 2001

Stratification effects by cohesive and noncohesive sediment

J. C. Winterwerp

Faculty of Civil Engineering and Geosciences, Delft University of Technology, Delft, Netherlands
WL/Delft Hydraulics, Delft, Netherlands

Abstract. This study focuses on stratification effects induced by the interaction between suspensions of fine-grained cohesive and noncohesive sediment and the turbulent flow in estuarine and coastal environments. A concise literature review reveals that this interaction may cause an appreciable modification of the vertical profiles of velocity, vertical eddy viscosity/diffusivity, and Reynolds stresses. This interaction is further studied with a one-dimensional vertical (1DV) numerical model, which includes the standard k-ε turbulence model with buoyancy destruction terms. Application of this model to the experimental results by *Coleman* [1981] shows that the measured changes in the velocity profile can be explained entirely by sediment-induced buoyancy effects. It is argued that when the carrying capacity for cohesive sediment is exceeded, a fluid mud layer is formed upon the deposition of the cohesive sediment flocs, contrary to the case with noncohesive sediment, where the depositing grains immediately form a rigid bed. Thus a two-layer fluid system develops causing significant damping of the vertical mixing processes, decreasing the carrying capacity further. This positive feed back results in a catastrophic collapse of the turbulence field and the concentration profile. A scaling law for this saturation behavior is derived from classical stratified flow theory. This law is sustained with a series of numerical experiments with the 1DV model. It also predicts the suspended sediment concentrations observed in the Yellow River to the right order of magnitude. It is concluded that sediment-induced buoyancy yields appreciable stratification effects at already moderate suspended sediment concentrations. In the case of cohesive sediment these stratification effects can result in a catastrophic collapse of the turbulent flow field and the vertical profile of suspended sediment concentration.

1. Introduction

The environment in many coastal and estuarine areas is characterized by the presence of large amounts of fine-grained cohesive and noncohesive sediment. The transport and fate of these sediments determine the bathymetry and stability of these areas, affect its water quality and ecological health through turbidity levels and adherence of contaminants and sediment composition, and are a nuisance to port authorities, who are often forced to undertake frequent maintenance dredging operations to safeguard navigation. Farther offshore, for instance, on continental shelves, large transports of sediment are encountered when the slopes of these shelves destabilize, generating huge turbidity currents.

Nowadays, engineers and scientists commonly use three-dimensional numerical models to study and predict the transport and fate of these fine-grained sediments. An important issue in such models is the interaction between the suspended sediment and the turbulent water movement. The present paper describes a study on this interaction in open-channel flow, discussing its implications and modeling requirements.

The water-sediment mixture is treated as a single-phase fluid in which all particles follow the turbulence movements except for their settling velocity. *Uittenbogaard* [1994] argues that this is a correct assumption if $w_s \ll w'_{\mathrm{RMS}}$, where w_s is the settling velocity of the sediment and w'_{RMS} is a measure for the (RMS value of the) vertical turbulent velocity fluctuations. Because w_s is of the order of 0.1–1 mm/s for fine-grained sediment and $w'_{\mathrm{RMS}} \approx u_*$ in open-channel flow [*Nezu and Nakagawa*, 1993], where u_* is the shear velocity with typical values of several centimeters per second, this condition is generally met in estuarine and coastal waters. It is noted that the well-known Rouse number $\beta = w_s/\kappa u_*$, where κ is the Von Kármàn constant, appears to be a proper parameter to establish whether a sediment suspension may be treated as a single-phase fluid.

Uittenbogaard [1994] showed theoretically that even sand particles with a diameter up to 200 μm can properly follow the turbulent movements typically occurring in tidal flows. This is sustained by *Muste and Patel* [1997] who measured the fluctuating velocity components of suspended sand particles of 250 μm median diameter in a turbulent flow and concluded that their RMS value is only ~15–20% smaller than the RMS values of the fluctuating fluid velocity components. Hence it is concluded that suspensions of fine-grained sediment in estuarine and coastal environments can indeed be treated as single-phase fluids.

In this study, distinction is made between the behavior of noncohesive and cohesive sediments. Noncohesive particles form a rigid bed upon deposition, at which turbulence production is always possible. As a result, an equilibrium condition exists, also referred to as capacity flow, which is the basis of many sediment transport formulae. In the case of cohesive sediment a very soft bed, or a layer of fluid mud if the amount of suspended sediment is large enough, is formed upon deposition as a result of the flocculation processes characteristic for cohesive sediment [e.g., *Winterwerp*, 2001a]. At the water-mud

Paper number 2000JC000435.
0148-0227/01/2000JC000435$09.00

interface, little or no turbulence production is possible, and no equilibrium concentrations are observed.

The present paper describes a part of an integral study on the behavior of high-concentrated mud suspensions [*Winterwerp*, 1999]. It discusses the interaction between the turbulent flow field and noncohesive sediment in stationary open-channel flow through a brief analysis of the literature in section 2 and the interaction of the flow with cohesive sediment in section 3. An analysis of the behavior of noncohesive and cohesive sediment from a conceptual point of view is given in section 4. The governing equations for both types of sediment are given in section 5. These equations are implemented in a one-dimensional vertical (1DV) point model, which is used to study the behavior of suspensions of noncohesive and cohesive sediment in open-channel flow; the results are described in sections 6 and 7; a discussion of the results and the conclusions of the present study are given in section 8.

2. Stratification by Noncohesive Sediment: A Literature Review

Many (experimental) studies have been published on the effect of suspended noncohesive sediment, i.e., sand, on the vertical velocity profile in turbulent open-channel flow. The two classical papers by *Vanoni* [1946] and *Einstein and Chien* [1955] are generally referenced. Vanoni executed experiments for hydraulically rough flow in a flume of 18 m length, 0.85 m width, and 0.15 m water depth with sand of 90, 120, and 147 μm median diameter. During the experiments, no sand was allowed to settle on the bed. Vanoni established the effective Von Kármàn constant κ_s for sediment-laden flow from the slope of the velocity profile in the lower 50% of the water column and concluded that κ_s decreases with increasing suspended sediment concentration c. Vanoni hypothesized that this decrease is caused by buoyancy effects, i.e., the damping of turbulence by the suspended sediment. Almost 10 years later, Einstein and Chien reported on their experiments for hydraulically rough flow in a flume of 13.3 m length, 0.3 m width, and 0.12 m water depth with sand of 94, 274, and 150 μm median diameter. The suspended sediment concentrations were much larger than Vanoni's. Again no sediment is allowed to settle on the bed. Also Einstein and Chien found decreasing κ_s values with increasing c.

Gelfenbaum and Smith [1986] reanalyzed the experimental data of *Vanoni* [1946] and *Einstein and Chien* [1955] with a semianalytical approach based on an empirical description of the eddy viscosity under neutrally buoyant conditions, the wave-current boundary layer description by *Grant and Madsen* [1979], and a reduction factor, which is a function of the local Richardson number, to account for turbulence damping by sediment-induced stratification effects. This approach yields a logarithmic vertical velocity profile with a reduced shear velocity (or reduced κ_s value) for concentration gradients in case of a critical value (1/4) of the Richardson number and a vertical profile of the suspended sediment concentration which simplifies to the well-known Rouse profile for neutrally buoyant conditions. From their analysis, Gelfenbaum and Smith concluded that a proper simulation of the experimental data required the inclusion of sediment-induced damping effects in their model.

The decrease in κ_s values with increasing c was well accepted in sedimentology until it was challenged by *Coleman* [1981, 1986], who argued that the logarithmic part of the velocity profile in open-channel flow is limited to the lower 10–20% of the water column. Higher in the water column the velocity profile is governed by the law of the wake. The analyses by *Vanoni* [1946] and *Einstein and Chien* [1955] would therefore be incorrect: the velocity distribution should be plotted in defect form. Coleman carried out a new series of laboratory experiments and reanalyzed the data of Vanoni and Einstein-Chien, using the velocity defect law. *Gust* [1984] pointed out in a fierce discussion of Coleman's work, that his analysis for sediment-laden flow is in fact based on one data point only. Later, *Valiani* [1988] also questioned the correctness of Coleman's conclusion on the basis of an error analysis of the data.

Itakura and Kishi [1980] also reanalyzed the experimental data of *Vanoni* [1946], *Einstein and Chien* [1955], and some others. They applied the Monin-Obukhov theory to establish a length scale for sediment-laden flows. This resulted in a log linear velocity defect profile, which may be viewed as a formulation with a linear wake profile. Their approach is therefore conceptually similar to *Coleman*'s [1981, 1986].

Lyn [1986, 1988] approached the sediment-flow interaction from another angle. He studied this interaction on the basis of "similarity theory," in which he assigned characteristic length, velocity, and concentration scales to the inner and outer parts of the flow. According to his experimental data and theoretical analysis the effect of the suspended sediment on the velocity profile is confined to approximately the lower 20% of the water column.

More theoretical approaches of the sediment-flow interaction were presented by *Hino* [1963] and more recently by *Zhou and Ni* [1995]. Hino's work was aimed at explaining the reduction in κ_s as a function of the suspended sediment concentration in turbulent flow, including observations by *Elata and Ippen* [1961] that a suspension of neutrally buoyant particles also causes a reduction in κ_s together with an increase in turbulent intensities. His analysis started from the turbulent energy equation for clear water flows. The effect of sediment would be the addition of a buoyancy term to account for the energy required to keep the particles in suspension and a reduction coefficient in the dissipation term. After some tuning of the various model coefficients, Hino was able to reproduce the velocity profiles measured by *Vanoni* [1946] and by Elata and Ippen. However, it is noted that the experiments by Elata and Ippen were not carried out with neutrally buoyant particles, but with 100–150 μm dylene polystylene particles with a specific density of 1.05 and a settling velocity of ~0.1 cm/s. Though specific density and settling velocity are much smaller than for common sand, this does not imply that buoyancy effects are negligible for the polystylene particles. In fact, it is expected that they are as important as for flocs of cohesive sediment (e.g., see sections 3 and 7).

Zhou and Ni [1995] carried out a perturbation analysis on the mean flow components of the Reynolds stress equations and the continuity equations for the fluid and the sediment; it was assumed that the turbulent flow fluctuations are not affected by the presence of sediment. The sediment-flow interaction was accounted for by an additional force term in the Reynolds stress equations. They showed that the zeroth-order approximation of the perturbation equation for the flow yields a logarithmic velocity distribution. The zeroth- and first-order approximations of the perturbation equation for the concentration distribution yielded a Rousean profile and the profile found by *Itakura and Kishi* [1980], respectively. The effect of

the sediment on the flow profile to first order appeared to be a parabolic mean flow profile superposed on the turbulent flow profile. This would result in a more laminar-flow-like velocity profile with a subsequent decrease in effective κ. They compared a linearized form of their perturbation equations with experimental data reported in the literature [*Coleman*, 1981; *Einstein and Chien*, 1955] and found good agreement after tuning two coefficients in the linearized equation. It is noted that this linearized form can be regarded as a defect law with a quadratic wake function.

It is remarkable that in the discussion on the effective Von Kármàn constant only a few authors refer in their analyses to studies on heat- and/or salinity-induced stratification effects; see, for instance, *Turner* [1973]. *Barenblatt* [1953] was probably the first to elaborate on this analogy. Barenblatt introduced the Monin-Obukhov length scale l to establish a damping function for the eddy viscosity, which resulted in log linear velocity profiles. This work was further elaborated by *Taylor and Dyer* [1977] in order to establish the effect of various flow and sediment properties on the velocity profile.

Also, the approach by *Gelfenbaum and Smith* [1986], as described above, models the sediment-turbulent flow interaction by introducing a damping function to the eddy viscosity profile. This approach was applied to the analysis of data on high-concentrated suspensions as observed on the Columbia River Shelf at water depths of ~50–140 m [*Kachel and Smith*, 1989] and the San Francisco continental shelf at water depths between 60 and 70 m [*Wright et al.*, 2001; *Wiberg et al.*, 1994] during storm periods. The sediment bed consisted of a mixture of clay, silt, and sand, which generated a suspension with a noncohesive behavior, as the clay concentration in the water column remained fairly low. It was shown that during storm periods, sediment-induced stratification effects become important and can be properly described with the proposed damping function. The wave boundary layer appeared to be affected mainly by the coarser sediment fraction, whereas the current boundary layer is affected by the finer sediment fractions. The results also suggest that the upper limit of sediment that can be contained within the current boundary layer under energetic waves is set by the vertical concentration gradient. This would imply a self-regulating process through positive feedback between vertical mixing capacity and settling flux. This self-regulating mechanism was also proposed by *Trowbridge and Kineke* [1994].

Further work was presented by *Soulsby and Wainwright* [1987] in the form of a stability diagram based on the Monin-Obukhov stability parameter $M_\zeta = z/l$, where z is the vertical coordinate. Stratification effects would be negligible if $M_\zeta < 0.03$. This diagram was more or less validated with some data from the Thames and the North Sea for suspended sediment concentrations ranging from ~10 to 10,000 mg/L. They concluded that in suspensions of fine sediments, stratification effects always commence in the upper part of the water column.

The above discussions are restricted to the effects of suspended sediment on the mean velocity profile with some indirect deduction of their effects on the turbulent flow properties. Only *Muste and Patel* [1997] carried out detailed measurements of the turbulent velocity intensities as a function of suspended sediment concentration. Their experiments were done for hydraulically rough flow in a flume of 30 m length, 0.91 m width, and 0.13 m water depth and with a concrete bottom. Various amounts of sand, sieved to a 210–250 μm diameter interval, were injected into the flume; no deposition on the bed was allowed. Though no data on the suspended sediment concentrations are given in their paper, depth-averaged values for the three series of experiments are estimated at ~100, ~200, and ~400 mg/L. Detailed laser Doppler velocity measurements revealed no significant effect of the suspended sediment on the RMS values of the horizontal and vertical velocity fluctuations of the fluid. The measured velocity fluctuations of the sediment particles themselves, however, were some 15–20% smaller than that of the flow throughout the depth. Muste and Patel concluded that these experiments do not provide evidence for sediment-induced turbulent damping effects, as this would also affect the turbulent flow properties. Apparently, the major effect in their experiments is the inability of the sand particles to follow the turbulent flow fluctuations completely.

Recently, *Cellino and Graf* [1999] published the results of a detailed experimental study on the influence of suspended sediment on the turbulence properties of open-channel flow. These experiments were carried out with 135 μm sand under hydraulically rough conditions in a 16.8 m long and 0.6 m wide flume at a water depth of 0.12 m. Depth-averaged flow velocities varied between ~0.73 and ~0.85 m/s, and the suspended sediment concentration was increased from clear water values (noncapacity or starved bed experiments) in small steps to capacity conditions over a sand bed at a depth-averaged concentration of ~4 g/L. Suspended sediment concentrations were measured by isokinetic sampling, and mean and turbulent-fluctuating velocities were measured acoustically. These measurements revealed that the Reynolds stress profile retained a linear form (also for capacity flow) but that the turbulent intensities themselves decreased appreciably with respect to clear water values. The vertical profile of suspended sediment concentration became more stratified with increasing sediment load. The vertical eddy diffusivity, finally, appeared to decrease by ~50% for capacity flow with respect to clear water conditions.

A very elegant experiment was performed by *Lau and Chu* [1987] in a tilting flume of 22 m length and 0.67 m width, at a water depth of 0.16 m and a flow velocity of ~1 m/s. They measured the vertical mixing rate of a passive tracer (10 parts per thousand (ppt) salt, made nonbuoyant with methanol) in clear water and sediment-laden flow, at sediment concentrations of 1 and 5 g/L. From these measurements they deduced a reduction in vertical eddy diffusivity by 57 and 73% for the tests with sediment and attributed this reduction to turbulence damping by sediment-induced buoyancy effects.

From this concise survey it is concluded that at present, no full consensus exists on the effects of suspended sediment on the vertical velocity profile and the turbulence properties. However, the results and conclusions by *Gelfenbaum and Smith* [1986], *Lau and Chu* [1987], and *Cellino and Graf* [1999] are more convincing than those by *Coleman* [1981], *Muste and Patel* [1997], and *Lyn* [1986]. In this study the hypothesis is therefore adopted, and further elaborated, that in the flow regime encountered in estuarine and coastal areas the interaction between fine-grained sediment and the turbulent flow is mainly governed by sediment-induced buoyancy effects.

3. Stratification by Cohesive Sediment: A Literature Review

Contrary to noncohesive sediment, the literature contains only a few studies on the interaction between cohesive sedi-

ment and the turbulent flow field. Detailed turbulence measurements were carried out by *van der Ham* [1999] and *van der Ham et al.* [1998] in the major channel of the Dollard estuary (the "Grote Gat") in the Netherlands, an estuary with a tidal range of 3–4 m. They measured the mean values and turbulent fluctuations of flow velocity and suspended sediment concentrations at various heights at concentrations of a few hundred to a few thousand milligrams per liter, and they found that the vertical turbulence structure (i.e., the turbulent stresses, the vertical transport, and the flux Richardson number) is affected significantly by the suspended sediment.

Adams et al. [1990] reported on a series of observations of the vertical sediment concentration distribution in a drainage channel in the Namyang Bay tidal flats on the west coast of South Korea. This area is characterized by strong tidal effects with a tidal range of 4.9 and 7.7 m for neap and spring tide, respectively, with peak spring values up to 9 m. The observations were made during ebb tide at a water depth of ~4 m. Continuous measurements of current speed and turbidity revealed a depth-averaged velocity of ~0.6 m/s with a strong gradient around a lutocline of 1 m thickness, and suspended sediment concentrations of the order of 1 g/L in the highly turbulent layer below the lutocline. Only little sediment was found in the upper layer. This highly stratified structure is characterized by a gradient Richardson number $Ri_g \approx 0.33$ and by pronounced interfacial waves with high-frequency Kelvin-Helmholz billows filling the entire water depth.

West and Oduyemi [1989] measured mean and fluctuating velocity components and sediment concentrations in the Tamar and Conway estuaries in the United Kingdom at neap, intermediate, and spring tide conditions with water depths varying between 1 and 5 m and suspended sediment concentrations ranging from 50 to 4000 mg/L. From these measurements they deduced reductions in the vertical turbulent momentum flux by ~80% at Richardson numbers beyond 0.3–0.5 and reductions in the vertical turbulent sediment flux up to 90% at Richardson numbers up to unity. The difference in damping between the vertical fluctuating momentum and sediment flux was attributed to the role of internal waves, which contribute to the velocity fluctuations but not to vertical mixing [see also *Uittenbogaard*, 1995b].

Reports were made on the sediment dynamics in the macrotidal South Alligator River by *Wolanski et al.* [1988] and the mesotidal Normanby estuary by *Wolanski et al.* [1992] in Australia. Both rivers show high concentrations, varying between 1 and 6 g/L. In their analysis, *Wolanski et al.* [1988, 1992] focused on the vertical exchange processes and stressed the important role of sediment-induced buoyancy effects on the vertical turbulence structure. *Wolanski et al.* [1992] emphasized the influence of high suspended sediment concentrations on the sediment-induced anisotropy of the turbulence, referring to field observations on the limited vertical mixing of turbidity currents with ambient water.

The results of the 2-year Amazon Sediment Studies (AMASEDS) campaign, covering low, rising, high, and falling river flow on the Amazon continental shelf, including a part of the Amazon mouth, have been reported in a series of papers [*Kineke*, 1993; *Trowbridge and Kineke*, 1994; *Kineke and Sternberg*, 1995; *Kineke et al.*, 1996]. Detailed measurements over the water depth of suspended sediment, flow velocity, salinity, and temperature were carried out at numerous locations; unfortunately, no data were collected on settling velocity or wave activity. This study revealed the importance of fresh saline water induced gravitational circulations on the horizontal sediment transport processes and the accumulation of the sediments forming a turbidity zone and of the role of the spring-neap tidal cycle in establishing the settling and mixing processes in the water column. Huge patches of fluid mud with concentrations of several tens to several hundred grams per liter were observed, and almost the entire survey area, covering about 300 by 500 km^2, revealed suspended sediment concentrations in the water column of the order of many hundreds of milligrams per liter to a few grams per liter. In their analysis, *Kineke et al.* [1996] stress the roles of vertical stratification, induced both by the river flow and the sediment suspension, and of the hindered settling processes on the sediment dynamics.

From this concise review it is concluded that buoyancy effects induced by cohesive sediments are appreciable in many cases. However, few quantitative analyses are presented in literature.

4. Behavior of Noncohesive and Cohesive Sediment

Suspensions of noncohesive sediment under steady state conditions are characterized by equilibrium concentrations, which are a measure for the sediment-carrying capacity of the flow. A decrease in flow velocity (or an increase in sediment load) will result in the settling of a part of the load. The depositing grains immediately form a rigid bed, at which turbulence production remains possible, and the rest of the sediment can be kept in suspension. Hence a (gradual) decrease in flow velocity will result in a (gradual) decrease in the sediment carrying capacity of this flow. This is elaborated in all textbooks on sediment dynamics.

For cohesive sediment a completely different picture emerges. Consider a sediment-laden flow over a rigid, horizontal bed with an amount of cohesive sediment equal or close to the flow's sediment-carrying capacity. When the flow velocity decreases slightly, sediment starts to settle, not to form a rigid bed but, as a result of flocculation processes [*Winterwerp*, 2000a], a layer of fluid mud, thus creating a two-layer fluid system. At the interface between the two layers, vertical turbulent mixing is damped strongly, decreasing the sediment-carrying capacity in the upper part of the flow further. This results in a snowball effect with a catastrophic collapse of the vertical turbulence field and the vertical sediment concentration profile. In this study, the suspended sediment concentration for cohesive sediment just prior to this collapse is denoted by the term "saturation concentration" to distinguish it from the equilibrium concentration for sand.

The first ideas on the existence of such a saturation concentration for cohesive sediment were presented by *Teisson et al.* [1992]; however, at that time, no explicit physical meaning was attributed to this parameter. The concept of the saturation concentration for cohesive sediment is based on empirical evidence [e.g., *Turner*, 1973] that a turbulent shear flow field collapses when the flux Richardson number Ri_f exceeds a critical value $Ri_{f,cr}$. Ri_f follows from the turbulent kinetic energy equation and is defined as the ratio of the buoyancy destruction and production term (e.g., section 5):

$$Ri_f = -\frac{g\overline{w'\rho'}}{\rho\overline{u'w'}\partial u/\partial z} = -\frac{\Delta g\overline{w'c'}}{\rho\overline{u'w'}\partial u/\partial z}, \qquad (1)$$

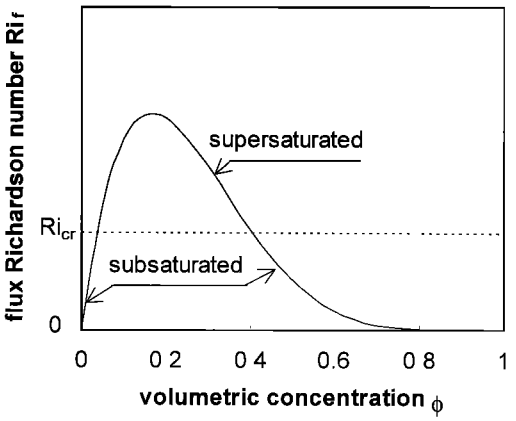

Figure 1. Schematic variation of the flux Richardson number with volumetric concentration.

where a prime denotes the fluctuating part of the horizontal and vertical velocity components u and w, of the density of the water-sediment suspension ρ, and of the suspended sediment concentration c, g is the gravitational acceleration, z is the vertical coordinate (positive upward), and Δ ($\Delta = (\rho_s - \rho_w)/\rho_s$) is the relative excess sediment density. The overbar denotes averaging over the turbulent timescale.

Starting the evaluation of sediment-laden flow at low (i.e., subsaturated) concentrations, a zeroth-order approximation is justified, in which the eddy diffusivity is only slightly affected by buoyancy. By assuming a logarithmic velocity profile ($\partial u/\partial z = u_*/\kappa z$), the corresponding parabolic viscosity profile ($\nu_T = \kappa u_* z(1 - z/h)$), local equilibrium between settling and mixing ($\overline{w'c'} = -w_s c$), and taking into account hindered settling effects (equation (12)), equation (1) can be elaborated to

$$Ri_f \propto \frac{\rho_s - \rho_w}{\rho_w} \frac{ghW_s c}{u_*^3} (1 - \phi)^5, \tag{2}$$

where ϕ is the volumetric concentration of the suspended sediment, equal to c/c_{gel}, with c_{gel} the gelling concentration, i.e., the concentration at which a space-filling network develops, and W_s is a reference settling velocity. The gelling concentration c_{gel} depends on the processes of fluid mud formation and can be established with a flocculation model. From in situ observations, c_{gel} appears to of the order of several tens to about a hundred grams per liter [e.g., *Winterwerp*, 2000a]. For given, but not specified, hydrodynamic conditions the variation of Ri_f as a function of ϕ is sketched in Figure 1, showing that Ri_f first increases with increasing ϕ and then decreases. The latter pattern is caused by the hindered settling effects.

At a specific level in the water column, Ri_f can exceed $Ri_{f,cr}$, upon which the turbulent field above this level collapses. In this study such conditions are referred to as supersaturation. The first part of the curve refers to subsaturated conditions, which are characterized by a measurable, but not yet fatal, interaction between the suspended sediment and the turbulent flow field. It is noted that such subsaturated conditions are also expected at very high suspended sediment concentrations, which occur, for instance, in turbidity currents generated from fluidization or liquefaction of consolidated deposits, for instance, as a result of geomechanical failure at the continental slope or of wave-induced liquefaction of coastal mud banks.

Substitution of the assumption of a logarithmic velocity profile into (1), as described in the discussion preceding (2), yields a relation for the vertical concentration profile c_s at the critical Richardson number:

$$c_s(z) = \frac{Ri_{f,cr}\rho}{\Delta g \kappa} \frac{u_*^3}{hw_s} \left(\frac{h}{z} - 1\right), \tag{3}$$

where u_* is the shear velocity, h is the water depth, and w_s is the local, effective settling velocity.

An extensive review of the collapse of turbulence in stratified flow is presented by *Hopfinger* [1987], who discusses laboratory experiments, oceanographic observations, and numerical simulations. His analysis focused on the development of the various length scales relevant for turbulent stratified flow, and he concluded that the onset of collapse occurs when the turbulence integral length scale becomes of the order of the buoyancy length scale.

Turner [1973] analyzed the experimental data of *Ellison* [1957], and several others, obtained from experiments in laboratory flumes and observations in the atmosphere, and concluded that a collapse of turbulence occurs when the flux Richardson number Ri_f attains critical values between 0.05 and 0.3, with an average value $Ri_{f,cr} \approx 0.15$. This value is close to the value given by *Tennekes and Lumley* [1994], who advocate $Ri_{f,cr} \approx 0.2$.

As $c_s(z)$ represents a vertical profile, a more convenient parameter is the depth-averaged saturation concentration C_s, which can also be regarded as a scaling parameter for saturated suspensions [e.g., *Galland et al.*, 1997]:

$$C_s \equiv \frac{1}{h} \int_0^h c_s \, dz = K_s \frac{\rho}{\Delta g} \frac{u_*^3}{hW_s}, \tag{4}$$

where K_s is a proportionality parameter. This scaling relation is further elaborated in section 7. At depth-mean concentrations beyond C_s (supersaturated) the turbulence collapses, and the flow is not able to carry the sediment in suspension. Hence C_s is a measure for the sediment load that can be carried by the turbulent flow.

It is interesting to note that this relation is very similar to the so-called Knapp-Bagnold criterion [*Parker et al.*, 1986] for the occurrence of submarine turbidity currents:

$$C < \frac{\rho}{\Delta g} \frac{U_t u_*^2}{\delta W_s}, \tag{5}$$

where U_t is the mean flow velocity of the turbidity current and δ is its thickness. This would be the necessary condition for a self-sustaining turbidity current; it is also known as the autosuspension criterion.

5. Equations Governing Sediment-Laden Flow

The transport of fine-grained sediment in estuaries and coastal waters is described with the continuity equation for the water phase, the momentum equation, the mass balance equation for the suspended sediment, a turbulence closure model, an equation of state, relating fluid density and suspended sediment concentration (and water temperature and salinity), and the appropriate boundary conditions. As this study is focused on the processes in the vertical, the three-dimensional equations are simplified to one (vertical) dimension only. These equations are implemented in the 1DV Point Model. This model is based on Delft Hydraulics' full three-dimensional

hydrostatic code DELFT3D, in which all horizontal gradients have been stripped, except for the longitudinal pressure gradient. Various versions are operational; here the version for fine-grained suspended sediment is used. For details, the reader is referred to *Winterwerp* [1999].

The horizontal momentum equation in the 1DV Point Model reads

$$\frac{\partial u}{\partial t} + \frac{1}{\rho}\frac{\partial p}{\partial x} = \frac{\partial}{\partial z}\left\{(\nu + \nu_T)\frac{\partial u}{\partial z}\right\} - \frac{1}{\rho}\frac{2\tau_{sf}}{b}, \tag{6}$$

where p is the pressure, $u(z, t)$ is the horizontal flow velocity, x and z are the horizontal and vertical coordinates, t is time, ρ is the fluid bulk density, ν is the kinematic viscosity, $\nu_T(z, t)$ is the eddy viscosity, including the effects of wind and/or waves, τ_{sf} is the possible wall shear stress, and b is the width of the channel. The pressure term in (6) is adjusted to maintain a given time-varying depth-averaged flow velocity:

$$\frac{1}{\rho}\frac{\partial p}{\partial x} = \frac{\tau_s - \tau_b}{\rho h} - \frac{2\tau_{sf}}{\rho b} + \frac{U(t) - U_0(t)}{T_{\text{rel}}},$$

$$U(t) = \frac{1}{h}\int_{z_{bc}}^{\zeta} u(z, t)\, dz, \tag{7}$$

where h is the water depth, U is the actual computed depth-averaged flow velocity, U_0 is the desired depth-averaged flow velocity, T_{rel} is a relaxation time, z_{bc} is the apparent roughness height, τ_b is the bed shear stress, τ_s is a possible surface shear stress, and ζ is the surface elevation. A quadratic friction satisfying the log law is used, and the boundary conditions to (6) read

$$\tau_b = \left\{\rho(\nu + \nu_T)\frac{\partial u}{\partial z}\right\}\Big|_{z=z_{bc}}; \qquad \tau_s = \left\{\rho(\nu + \nu_T)\frac{\partial u}{\partial z}\right\}\Big|_{z=\zeta}. \tag{8}$$

For hydraulically rough conditions the apparent roughness height is prescribed at the bed, whereas for hydraulically smooth conditions the friction coefficient is determined as a function of the flow Reynolds number by the Kármàn-Schoenherr equation.

The effect of waves on the bed shear stress and the vertical mixing is modeled through the approach of *Grant and Madsen* [1979] in the form of an additional bed boundary condition to the flow model, applying linear wave theory to relate wave length and period, and orbital excursion and velocity. This approach gives good results for larger wave activity, but for smaller waves the wave effect is overestimated by ~20% [e.g., *Soulsby et al.*, 1993]. Details on this approach in the 1DV point model are given by *Winterwerp et al.* [2001].

Uittenbogaard [1995a] has shown that the k-ε turbulence closure model is applicable to fairly stratified conditions. This model, with a sediment-induced buoyancy term, is therefore used. This model was also applied fairly successfully by *Fukushima and Fukuda* [1986] simulating the laboratory experiments by *Vanoni and Nomicos* [1960].

Burchard and Baumert [1995] tried to establish $Ri_{f,cr}$ for stratified flow from an analysis of the k-ε equations. They neglected the diffusion term and, after some further simplifying assumptions, were able to derive an analytical solution. From this analysis they concluded that the k-ε equations can describe the collapse of turbulence in a stratified flow, as described by *Hopfinger* [1987].

Hence it is concluded that the k-ε turbulence model is applicable for sediment-laden turbulent flow. Its standard version [e.g., *Rodi*, 1984] is therefore implemented in the 1DV Point Model; it consists of transport equations for the turbulent kinetic energy k and the turbulent dissipation per unit mass ε, neglecting horizontal transport components:

$$\frac{\partial k}{\partial t} = \frac{\partial}{\partial z}\left\{(\nu + \Gamma_T^{(k)})\frac{\partial k}{\partial z}\right\} - \overline{u'w'}\frac{\partial u}{\partial z} - \frac{g}{\rho}\overline{\rho'w'} - \varepsilon \tag{9a}$$

$$\frac{\partial \varepsilon}{\partial t} = \frac{\partial}{\partial z}\left\{(\nu + \Gamma_T^{(\varepsilon)})\frac{\partial \varepsilon}{\partial z}\right\} - c_{1\varepsilon}\frac{\varepsilon}{k}\overline{u'w'}\frac{\partial u}{\partial z} - (1 - c_{3\varepsilon})\frac{\varepsilon}{k}\frac{g}{\rho}\overline{\rho'w'} - c_{2\varepsilon}\frac{\varepsilon^2}{k}, \tag{9b}$$

where a prime denotes turbulent fluctuations and an overbar denotes averaging over the turbulent timescale. The turbulent transport terms are modeled as a diffusion process, and the eddy viscosity ν_T and eddy diffusivity $\Gamma_T^{(\varphi)}$ are given by

$$\nu_T = c_\mu \frac{k^2}{\varepsilon}; \qquad \Gamma_T^{(\varphi)} = \frac{\nu_T}{\sigma_T^{(\varphi)}}, \tag{10}$$

where σ_T is the turbulent Prandtl-Schmidt number for substance φ. Most coefficients in the k-ε turbulence model are well established and are the result of calibration against grid-generated turbulence and a log law velocity profile for homogeneous experiments.

The values of the Prandtl-Schmidt number σ_T and the coefficient $c_{3\varepsilon}$ are less well established. Here *Uittenbogaard* [1995a] is followed. He showed conclusively that in free turbulence, $\sigma_T = 0.7$, even under highly stratified conditions. Experimental data deviating from this value are explained in terms of the effects of internal waves, which do transfer momentum but not mass. This effect is generally accounted for by a modification of σ_T, which is often modeled as a function of the Richardson number itself. *Uittenbogaard* [1995a, 1995b], instead, promotes the use of additional terms in the k-ε model through which the effects of internal waves can be described explicitly. He also argued why $\sigma_T < 1$. In turbulent flow, packages of fluid are deformed continuously by the turbulent stresses in the fluid. The deformation of these packages, however, is restricted by the requirements of continuity: If the deformation in two directions is given at any time, then the deformation in the third direction follows from continuity. In other words, if $\partial u_1'/\partial x_1$ and $\partial u_2'/\partial x_2$ are given, $\partial u_3'/\partial x_3$ is set. This affects the value of the correlation between the turbulent velocity components. This restriction does not apply to a solute, as a solute can diffuse freely through the fluid. Hence the correlation between c' and u_i' has more degrees of freedom than the correlation between the turbulent velocity components themselves. As it was concluded that the particles of fine-grained sediment can be treated as a passive tracer (apart from its settling velocity) in a single-phase description; the argument above is also valid for the turbulent diffusion of the fine sediments in this study.

From an analysis of the experiments in stratified flow by *Lienhard and Van Atta* [1990], *Uittenbogaard* [1995a] also concluded that for stable stratified flows the buoyancy term in the ε equation vanishes ($c_{3\varepsilon} = 1$). For unstable stratified flow conditions, $c_{3\varepsilon} = 0$ is fair, which implies ε production, i.e., small-scale turbulence production, by Rayleigh-Taylor instabilities.

This analysis yields the following set of coefficients in the k-ε model:

$$c_\mu = 0.09, \quad c_{1\varepsilon} = 1.44, \quad c_{2\varepsilon} = 1.92,$$
$$\sigma_T^{(k)} = 1.0, \quad \sigma_T^{(\varepsilon)} = 1.3,$$
$$\sigma_T^{(\rho)} = 0.7, \quad \kappa = 0.41, \quad c_{3\varepsilon} = 1$$

for stable stratification. The model is closed with the following set of boundary conditions:

$$k|_{z=z_{bc}} = \frac{\mu_{*b}^2}{\sqrt{c_\mu}}, \quad \varepsilon|_{z=z_{bc}} = \frac{u_{*b}^3}{\kappa z_{bc}}, \quad k|_{z=\zeta} = 0, \quad \varepsilon|_{z=\zeta} = 0. \tag{11}$$

The transport of sediment is modeled with the advection-diffusion equation:

$$\frac{\partial c}{\partial t} - \frac{\partial}{\partial z}\{W_{s,ef}\, c\} - \frac{\partial}{\partial z}\left\{(D + \Gamma_T)\frac{\partial c}{\partial z}\right\} = 0, \tag{12a}$$

with

$$W_{s,ef} = W_{s,o}(1 - \phi)^\beta \tag{12b}$$

to account for hindered settling, where $W_{s,o}$ is the settling velocity of a single grain in still water and the exponent β generally has the value $\beta \approx 5$ for fine-grained sediment. The volume concentration ϕ in (12) is related to the mass concentration c through $\phi = c/\rho_{\text{ref}}$, where ρ_{ref} is either the density of massive sand particles (i.e., $\rho_{\text{ref}} = \rho_s \approx 2650$ kg/m^3) or, in case of muddy suspensions, the gelling concentration $\rho_{\text{ref}} = c_{\text{gel}}$, i.e., the sediment concentration at which a space-filling network is formed as a result of flocculation processes.

The boundary condition at the bed is given by a zero sediment flux or is prescribed either by the classical Krone-Partheniades formulae for cohesive sediment or by the formula of *van Rijn* [1987] for noncohesives. At the water surface a zero-flux boundary condition is prescribed. The buoyancy term in (9a) and (9b) accounts for the effect of vertical sediment and salinity gradients:

$$\rho(S, c) = \rho_w(S) + \left(1 - \frac{\rho_w(S)}{\rho_s}\right)c, \tag{13}$$

with $\rho_w(S)$ is the density of the water due to salinity only. These equations are solved on a so-called σ coordinate system. Time discretization is based on the θ method; for $\theta = 1$ the Euler implicit time integration method is obtained. The convection term is discretized by a first-order upwind scheme in conjunction with a three-point scheme for the diffusion operator.

The 1DV Point Model is validated, among other things, against analytical solutions of the vertical sediment concentration profile provided by *Malcherek* [1995], whose results are not presented here, and against measured vertical velocity and concentration profiles for sediment-laden flow in a straight flume as published by *Coleman* [1981], as shown in section 6.

6. Modeling Noncohesive Sediment Suspensions

In order to establish whether subsaturated suspensions can indeed be properly described with the single-phase approach and the standard k-ε turbulence closure model, the experiments carried out by *Coleman* [1981] to study the influence of suspended sediment particles on the velocity profile in open-channel flow were simulated with the 1DV point model. The experimental results were published in two papers. *Coleman* [1981] provides the primary data and analyses, and *Coleman* [1986] provides additional tables with the raw data and some additional analyses. Some further details were given in *Coleman*'s [1984] reply to *Gust*'s [1984] discussion of the results of *Coleman* [1981].

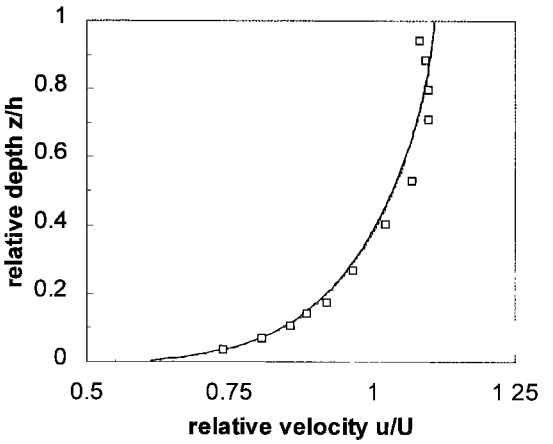

Figure 2. Simulation of *Coleman*'s [1981] clear water experiments: nondimensional velocity profiles.

The experiments were carried out in a tilting, recirculating flume with a plexiglass channel of 15 m length and 0.356 m width, operated at a water depth of ~0.17 m. The flow rate was measured with a venturi meter, the flow velocity with a traversible Pitot tube, the bed shear stress with a Preston tube, the surface slope with two point gauges 6 m apart, and the water temperature with a thermometer. Vertical profiles of the suspended sand concentration were also measured with the Pitot tube, deployed to withdraw isokinetic samples. The Pitot tube and Preston tube measurements were carried out in the centerline of the flume, 12 m downstream from the inlet. No data on experimental accuracy were given by *Coleman* [1981; 1984].

The sediment used was composed predominantly of quartz and feldspar; the finest sample had a diameter between 88 and 125 μm, with a median diameter of 105 μm, and its settling velocity is established from Stokes' law. The experiments with this finest sediment are analyzed in this section.

The bed and wall of the flume were smooth; no roughness elements were installed, and during the experiments, no sand was allowed to settle on the bed. All experiments were carried out at uniform flow conditions.

Unfortunately, the experimental data are probably biased by (strong) secondary currents and/or a meandering longitudinal flow: (1) the measured flow velocity decreases in the upper 30% of the water column, as shown in Figure 2, indicating that almost the entire upper half of the water column is affected by such secondary currents, and (2) the depth-mean value U of the flow velocity profile measured in the symmetry plane of the flume is ~10% smaller than the cross-sectional mean flow velocity U_Q obtained from the measured flow rate (see Table 1).

Despite these fairly strong secondary current effects, the data are suitable for analysis with the 1DV point model, as can be concluded from the successful simulations by *Galland* [1996] with a Reynolds stress model. Moreover, the author is

Table 1. Conditions of *Coleman*'s [1981, 1986] Experiments

Parameter	Symbol	Test 1	Test 10	Remarks
Flume Experiments				
Water depth, m	h	0.172	0.171	measured
Flow rate, m^3/s	Q	0.064	0.064	measured
Cross-sectional mean velocity, m/s	U_Q	1.05	1.05	from flow rate
Depth-mean velocity, m/s	U	0.96 ± 0.02	0.96 ± 0.02	by integration
Shear velocity, m/s	u_*	0.041	0.041	measured
Amount of suspended sand, kg		0	8:18	
Depth-mean concentration, g/L	C_m	0	6.0 ± 0.2	by integration
Settling velocity, mm/s	$W_{s,50}$	...	10.7	from Stokes
Bed friction coefficient	f	0.0149	0.0149	
1DV Simulations				
Relative grid size	$\Delta z/h$	0.01	0.01	
Time step, s	Δt	1	1	
Simulation period, s	T_{sim}	1000	1000	
Roughness		hydraulically smooth		
Buoyancy		...	yes/no	
Shear velocity, m/s	u_*	0.042	0.039/0.042	computed

not aware of any other data in the literature on sediment-laden flow with sufficient detail to carry out such analyses. For instance, *Vanoni* [1946] presents data in only the lower part of the water column, whereas the experiments by *Einstein and Chien* [1955] are carried out for hyperconcentrated conditions, where grain-grain interactions may affect the stress-strain relations.

In the following paragraphs the experiments by *Coleman* [1981, 1986] are used to analyze the effects of sediment-induced buoyancy on the vertical velocity and concentration profile and, indirectly, to test the 1DV Point Model. This is done with a series of numerical experiments with the model, using U as depth-mean velocity and a zero-flux boundary condition: (1) in the first series, Coleman's clear water experiments are simulated, including the effect of sidewall friction, (2) in the second series, Coleman's sediment-laden experiments are simulated (including sediment-induced buoyancy effects), and (3) in the third series the effect of sediment-induced buoyancy on the vertical velocity and concentration profile is explicitly studied.

First, Coleman's test 1 (clear water) experiment is simulated with the 1DV Point Model. The relevant numerical parameters are summarized in Table 1. Simulations are carried out with and without sidewall friction (e.g., equation (2)); however, the effect of sidewall friction appeared to be negligible.

The results for the clear water experiments are presented in Figure 2, showing fair agreement between simulations and data in the lower 20–30% of the water column. Higher in the water column the comparison becomes less favorable because of the effects of secondary currents, which are not accounted for in the numerical model. Note that the computed and measured shear velocity (see Table 1) agree within experimental accuracy, which supports the choice to use U instead of U_Q.

The computed and measured velocity profiles (second series) for the sediment-laden test 10 are presented Figure 3. It is observed that the agreement between computed and measured data near the wall in Figure 3 is slightly less than that in Figure 2. This will be elaborated below.

The agreement between computed and measured vertical suspended sediment concentration is fair (see Figures 4a (linear scales) and 4b (logarithmic scales)) and of the same quality as the results presented by *Galland* [1996]. An even better agreement can be obtained by tuning the settling velocity, but this was not done.

In the third series, simulations of test 10 conditions are carried out but without sediment-induced buoyancy effects. The results are presented in Figure 5a in log law form and in Figure 5b in defect law form; the effects on the vertical concentration profiles are presented in Figure 6. Here the following definitions have been used: $u_+ = u/u_*$, $z_+ = zu_*/\nu$, and Z_m is the level at which the maximal flow velocity U_m is observed. The computed velocity profile with sand but without buoyancy effects is, of course, identical to the computed clear water profile (e.g., Figure 2). Figures 5a and 6 clearly show that the sediment-induced buoyancy effects reduce the vertical mixing, as expected. This is also shown in Figure 7, where the computed eddy viscosity profiles with and without sand (buoyancy effects) are compared. This computed decrease in eddy viscosity is qualitatively similar to the decrease measured by *Cellina and Graf* [1999].

Figure 5a shows that near the bed and near the water surface the computed velocity profile is not entirely logarithmic. This is due to the Dirichlet boundary conditions of the k-ε equations, chosen to guarantee a robust numerical scheme. Note that the

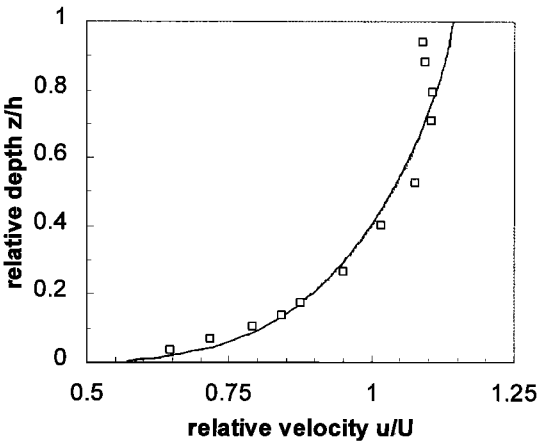

Figure 3. Simulation of *Coleman*'s [1981] sediment-laden experiment: nondimensional velocity profiles.

logarithmic scale in Figure 5a exaggerates this nonlogarithmic behavior near the wall; actually, only the lower four to five computational points deviate from a logarithmic profile. It is noted that preliminary tests have been carried out with a Neuman boundary condition. In this case the clear water velocity profile became indeed entirely logarithmic, but the overall behavior of the model, both for cohesive and noncohesive sediment, did not change. The results of these numerical experiments are not presented here.

Further, it is noted that the computed velocity profile for the sediment-laden test lies above the measured data, whereas it lies below the data for the clear water experiments (Figure 5a). This difference is entirely due to the difference in computed and measured shear velocity (e.g., Table 1).

Figure 5b on the contrary, showing the results in defect-law-form, is very illuminating. It is this form of presentation that inspired *Coleman* [1981] to his analysis of the effect of suspended sediment on the wake function of the velocity profile. Figure 5b clearly shows that the effect of suspended sand on the measured velocity profile is properly predicted by the simulations by including a sediment-induced buoyancy term in the turbulent energy equation of the numerical model. Comparison of the computed sediment concentration profile with and without buoyancy effects (e.g., Figure 6) clearly shows a considerable deviation from the measured data for the simulation without buoyancy effects.

From these analyses it is concluded that the 1DV Point Model is able to reproduce the major features of sediment-laden flow and that the effects of the suspended sediment on the velocity profile in open-channel flow is explained largely through sediment-induced buoyancy effects, as hypothesized by *Vanoni* [1946]. This analysis also agrees with the results by *Gelfenbaum and Smith* [1986].

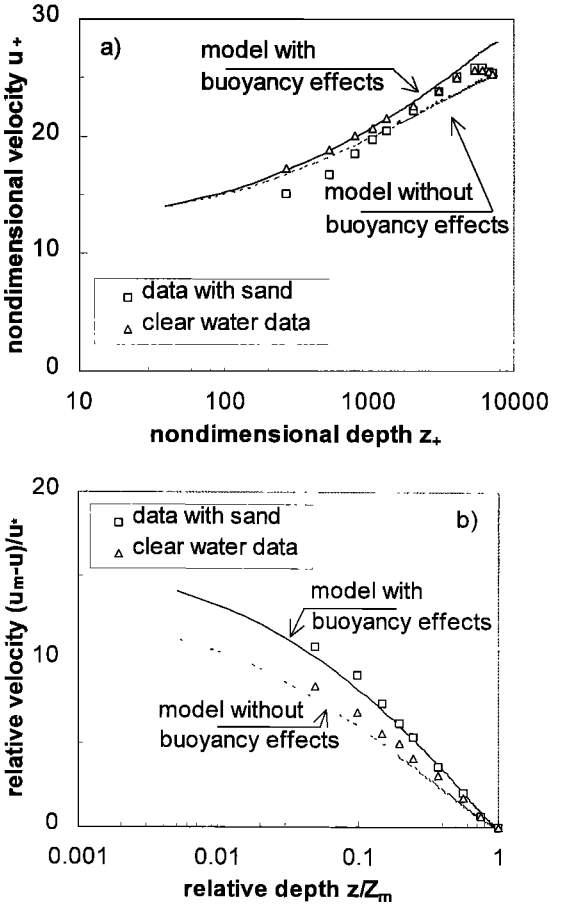

Figure 5. Sediment-induced buoyancy effects on velocity profile in (a) log law form and (b) defect law form.

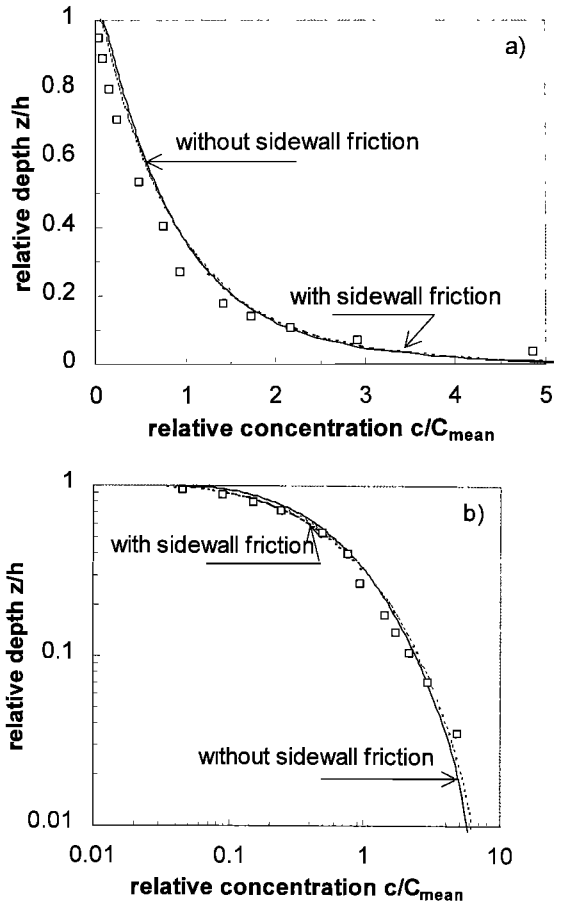

Figure 4. Simulation of *Coleman*'s [1981] sediment-laden experiment: sediment concentration profiles.

7. Modeling Cohesive Sediment Suspensions

The behavior of cohesive sediment suspensions is characterized by flocculation effects and the formation of fluid mud layers, hence a stratified two-layered fluid system, upon deposition of the flocs of cohesive sediment. This fluid mud formation is explicitly accounted for in the numerical model by the hindered settling formula and a proper choice [e.g., *Winterwerp*, 2000a] of the value of c_{gel}, in contrast to the situation for noncohesive sediment.

The saturation concept in section 3 is well illustrated by two simulations with the 1DV point model for a hypothetical open-channel flow of 16 m depth, a constant depth-averaged flow velocity of $U = 0.2$ m/s, and a constant settling velocity $W_s = 0.5$ mm/s. Initially, the sediment is distributed homogeneously over the water depth. The initial concentration C_0 was increased in small steps until saturation occurred. Other parameter settings are listed in Table 2. The grid size at the bed is set at $0.0002h$; the size of successive grids is increased by a factor 1.5 until a grid size of $0.01h$ is attained. The time evolution of the suspended sediment concentration in the form of isolutals (i.e., lines of constant sediment concentration) is shown in

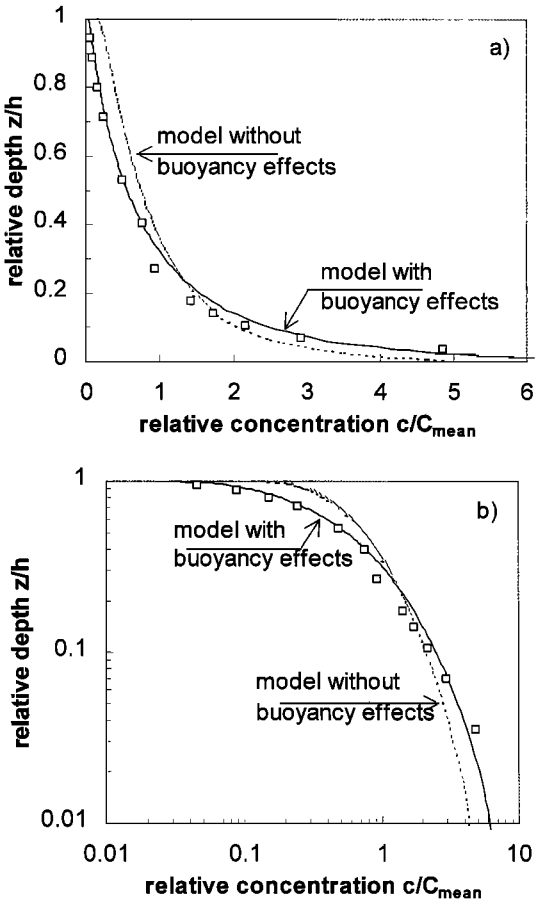

Figure 6. Sediment-induced buoyancy effects on vertical concentration profile.

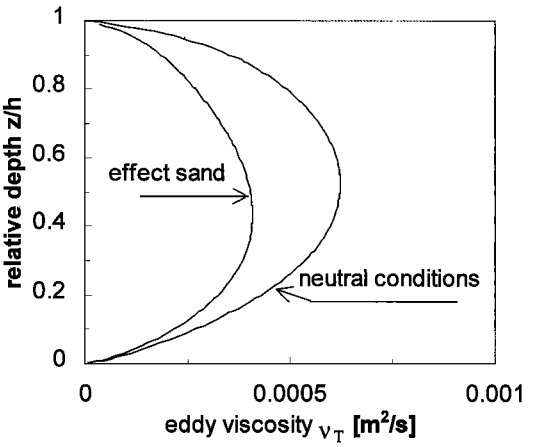

Figure 7. Computed eddy viscosity profiles.

Figure 8 for an initial concentration of $C_0 = 0.023$ g/L and in Figure 9 for $C_0 = 0.024$ g/L.

It is clear that the 0.023 g/L case represents saturation conditions: a small increase in C_0 results in a catastrophic collapse of the concentration profile, as shown in Figure 9. The final concentration profile in the 0.023 g/L case is more or less Rousean, whereas in the 0.024 g/L case a fluid mud layer is formed. The coefficient K_s (see equation (4)) appears to have a value of $K_s \approx 0.7$.

Figure 10 shows the time development of the vertical distributions of suspended sediment concentration and eddy diffusivity for the 0.024 g/L case (note the logarithmic scales). It is interesting to observe that the vertical profile at $t = 200$ min has two more or less parabolic curves: In the lower 80% of the water column, turbulence is still generated at the bottom and by the velocity shear, and the maximum value of the eddy diffusivity amounts to ~0.006 m^2/s. Around the interface at $z/h = 0.8$, Γ_T almost vanishes, whereas in the upper 20% of the water column, some mixing can occur again, induced by some interfacial stress and local velocity shear; the maximum value of the eddy diffusivity in this part of the water column amounts to ~0.001 m^2/s. This behavior becomes more pronounced during the remaining settling time.

From the various profiles it is observed that the eddy diffusivity in the upper part of the water column slowly collapses as a result of the damping induced by the buoyancy term in the turbulent energy equation. An equilibrium is obtained only after 3000 min. It is also observed that after 1000 min, when the majority of the sediment is deposited in the fluid mud layer, the eddy diffusivity profile is restored a bit because some turbulence can be produced by the shear flow in the water column, but it remains an order of magnitude smaller than in the nonbuoyant case ($t = 10$ min). Also, the bed shear stress decreases considerably: u_* decreases from 0.9 to 0.4 cm/s.

These results also imply that the sediment-carrying capacity of the flow decreases by an order of magnitude. This collapse is irreversible as long as the fluid mud layer remains soft, i.e.,

Table 2. Reference Parameter Settings in Numerical Simulations

Parameter	Symbol	Value	Remarks
Water depth, m	h	8 and 16	constant; also for tidal flow
Flow velocity	U	variable	steady state
Bed roughness, mm	z_0	1	hydraulically rough
Water density, kg/m^3	ρ_w	1020	
Sediment density, kg/m^3	ρ_s	2650	
Initial sediment concentration	C_0	variable	initial homogeneous profile
Settling velocity, mm/s	W_s	0.5	constant
Hindered settling		yes	
Gelling concentration, g/L	c_{gel}	80	
Water bed exchange		no	
Prandtl-Schmidt number	σ_T	0.7	
Number of layers		109	logarithmic/equidistant
Time step, min	Δt	1	
Relaxation time, min	T_{rel}	2	

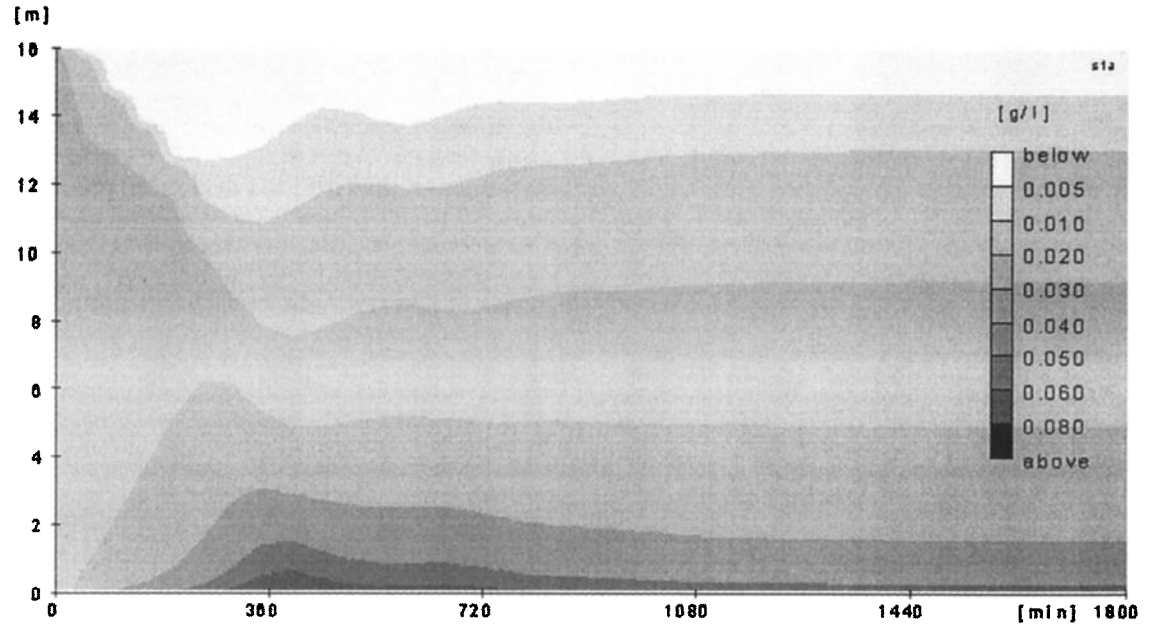

Figure 8. Isolutals for a saturated ($C_0 = 0.023$ g/L) suspension in open-channel flow.

as long as no yield stress builds up, so that no turbulence can be generated at the water-mud interface.

Next, a series of numerical simulations is carried out to verify scaling law (4). This is done, starting from subsaturated conditions, by increasing, for given hydrodynamic conditions, the initial sediment concentration in small steps until a collapse of the concentration profile is observed. The setting of the various parameters is given in Table 2. The results are presented in Figure 11, where the computed vertical flux $W_s C_s$ is plotted versus the mean flow velocity U. It is observed that the numerical results follow the functional relationship $W_s C_s \propto U^3$ properly. The influence of the time step and the number of layers is also studied and can be seen to be negligible.

Also the effects of a different value of the coefficient $c_{3\varepsilon}$ (i.e., $c_{3\varepsilon} = 0$) in the k-ε turbulence model (9) has been studied, which resulted in a (considerable) increase (several tens of percent) in the value of C_s, but the catastrophic behavior is maintained. The results of these simulations are not presented here.

Kranenburg [1998] also studied the saturation behavior of sediment-laden flow but with a Prandtl mixing length model. In this model, sediment-induced buoyancy effects are accounted for through Munk-Anderson-like damping functions, with slightly altered coefficients though. Also, Kranenburg observed a similar catastrophic behavior when increasing the sediment load in small steps. However, the actual saturation concentra-

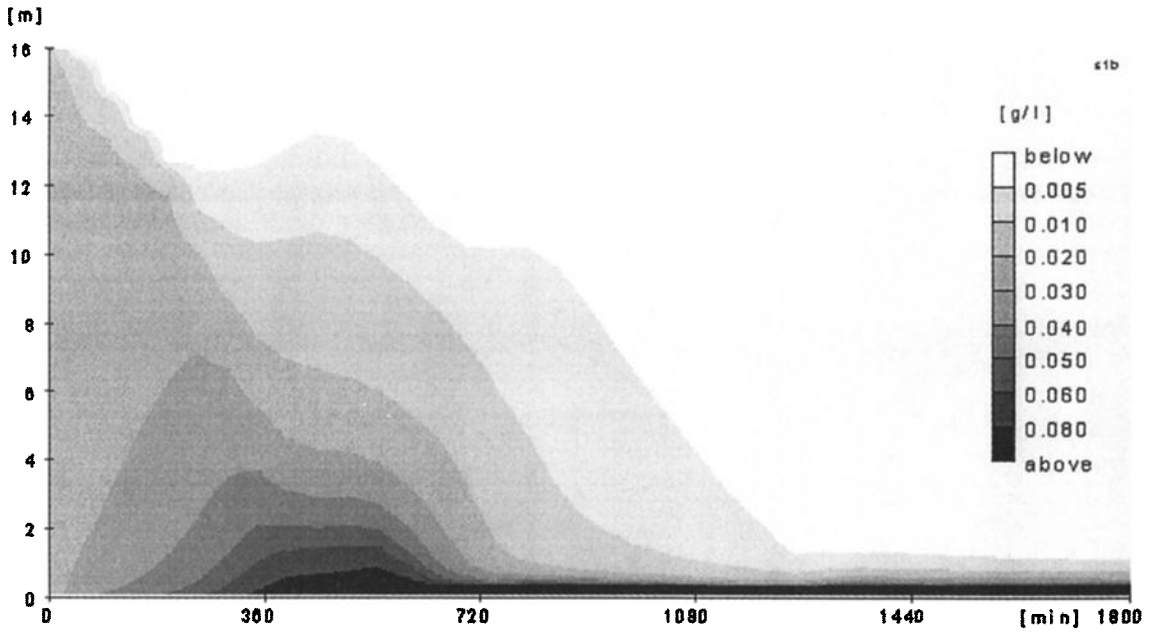

Figure 9. Isolutals for a supersaturated ($C_0 = 0.024$ g/L) suspension in open-channel flow.

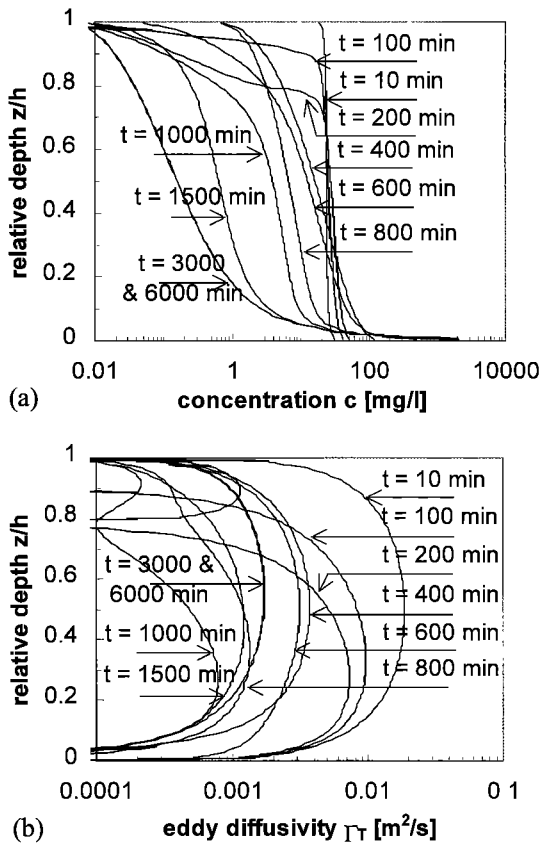

Figure 10. Concentration and eddy diffusivity profiles for $C_0 = 0.024$ g/L.

tion appeared to deviate slightly from the values obtained with the k-ε model.

This saturation behavior is also found for tidal conditions. The scaling laws in this case are rather different though [*Winterwerp*, 2001b]. It is argued that under tidal conditions such saturation behavior is fairly common in nature, especially in the turbidity maximum of estuaries.

A good candidate for the occurrence of saturated conditions for steady flow in nature is the Yellow River. Strong interactions between the sediment and the (turbulent) flow have been reported frequently [*Brush et al.*, 1989], among which are the occurrence of a completely flat water surface, indicating laminar flow conditions, and of plug flow, indicating viscoplastic behavior. The amount of sediment carried by the river is so large that its availability seems unlimited; hence it is expected that the sediment load will be close to the sediment-carrying capacity of the river.

Accurate data on the suspended sediment concentrations in the Yellow River are scarce. Data of *Wan and Wang* [1994] and *Qi et al.* [1993] are assumed to represent saturation values and are plotted in Figure 11. They show considerable scatter. However, the data are in the range predicted with the 1DV point model, thus qualitatively supporting the analyses in the preceding discussion.

The saturation concept also allows an analysis of the occurrence of mud banks in coastal areas, where wave effects are important. The erosive capacity of waves largely exceeds their mixing capacity. Hence one may expect that under storm conditions, coastal sites may become supersaturated when abundant amounts of mud are available in and mobilized from the seabed.

The mud in the seabed may be mobilized by liquefaction of the bed by the stresses induced by the waves [e.g., *de Wit*, 1995, *van Kessel*, 1997, and *Van Kesteren et al.*, 1997]. If this does not occur, the bed still may be eroded by wave-induced shear stresses at the bed. These generally exceed the flow-induced shear stresses by an order of magnitude. At present, only the latter process is accounted for in the 1DV Point Model. This, however, is sufficient for the present analysis.

Figure 12 presents the results of a simulation for a hypothetical case, showing the effect of 1.8 m waves on the suspended sediment concentration in steady state open-channel flow, initially containing no sediment. The various numerical parameters are summarized in Table 3.

Figure 12 shows that initially the suspended sediment concentration increases with time. However, after ~500 min the vertical concentration profile starts to collapse and a fluid mud layer is formed. In this period the current and flow-induced shear velocity decreases from 5.9 to 3.2 cm/s. However, it is doubtful whether the erosion mechanism under wave action is described properly by the classical Partheniades formulation, presently used in the 1DV Point Model. For instance, the simulation of Figure 12 predicts that the flow and waves continue to erode the seabed, as a result of which the amount of sediment in the fluid mud layer continues to grow. In reality, one would expect that the waves are damped by the fluid mud layer and that the underling bed becomes protected from further erosion [see also *Winterwerp et al.*, 2001].

However, from a conceptual point of view the picture sketched in Figure 12 seems realistic in the sense that the flow becomes supersaturated due to the wave action, forming a fluid mud layer. Such a result can only be obtained if sediment-induced buoyancy effects are included in the model. It is conjectured that this mechanism is responsible for the occurrence of the mud banks encountered in many coastal zones (e.g., Kerala coast, India; west coast of Korea; coast of Surinam).

8. Discussion and Conclusions

From an extensive literature survey it is concluded that the original consensus that the decrease of the effective Von Kármàn constant κ_s for sediment-laden flows is caused by sediment-induced buoyancy effects is challenged by some au-

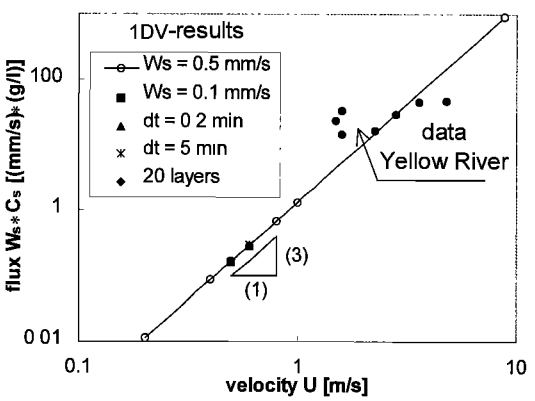

Figure 11. Saturation flux W_sC_s as a function of flow velocity (results from 1DV point model). Note that several symbols collapse because results are identical.

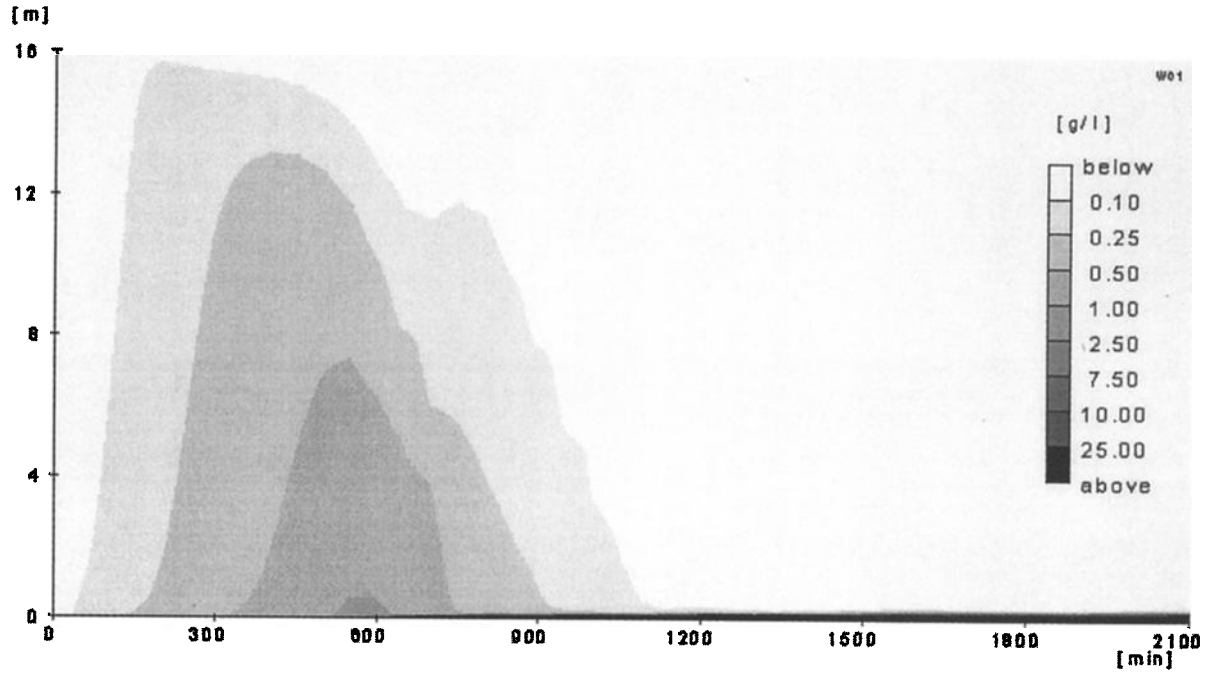

Figure 12. Autosaturation by wave action, results of 1DV simulation.

thors at present. The discussions in literature are especially focused on the question whether the effect of suspended sediment is restricted to the lower, near-bed part of the velocity profile or if it is also manifest higher in the water column. It should be borne in mind, though, that a steepening of the near-bed velocity gradients (decrease in κ_s) must be compensated by a decrease higher in the water column, when the flow rate is kept constant. Hence the driving agent of the flow (i.e., constant slope or constant flow rate) is a controlling parameter.

It is argued that fine-grained sediment suspensions can be treated as a single-phase fluid. This is further substantiated by a series of numerical experiment with the 1DV Point Model which consists of the momentum and advection-diffusion equations for a single-phase fluid, together with a k-ε turbulence closure model. Simulations of the laboratory experiments by *Coleman* [1981] yielded favorable results. These numerical simulations predicted that both the observed decrease in effective Von Kármàn constant and the observed modification of the velocity defect law are the result of sediment-induced buoyancy effects. It is noted that these effects become measurable at already fairly low concentrations, i.e., a few grams per liter (or ~0.1% volumetric concentration). Similar results have been published by *Gelfenbaum and Smith* [1986], analyzing laboratory experiments by *Vanoni* [1946] and *Einstein and Chien* [1955] with a semianalytical model, and by *Adams and Weatherly* [1981], analyzing the boundary layer of the Florida current using a Mellor-Yamada level II turbulence model.

Table 3. Parameter Settings 1DV Simulation of Wave-Induced Autosaturation

Parameter	Symbol	Value
Water depth, m	h	16
Flow velocity, m/s	U	0.5
Wave height, m	$H_{1/3}$	1.8
Mean wave height, m	H_{RMS}	1.3
Wave period, s	T_{RMS}	4.8
Bed roughness, m	z_0	0.001
Water density, kg/m^3	ρ_w	1020
Sediment density, kg/m^3	ρ_s	2650
Initial concentration, g/L	C_0	0
Settling velocity, mm/s	W_s	0.5
Gelling point, g/L	c_{gel}	80
Erosion parameter, kg/m^2 s	M	10^{-4}
Critical stress deposition, Pa	τ_d	0.5
Critical stress erosion, Pa	τ_c	0.1
Hindered settling		yes
Buoyancy		yes
Prandtl-Schmidt number	σ_T	0.7
Grid size	$\Delta z/h$	0.01
Time step, min	Δt	1.0
Relaxation time, min	T_{rel}	2.0

This single-phase approach allows a comparison with well-established theory for salinity- and/or temperature-induced stratification effects. This led to a conceptual diagram which shows that for a given flow field the flux Richardson number Ri_f first increases with increasing suspended sediment concentration and then decreases at even larger concentrations. The latter is the result of hindered settling effects. Ri_f may exceed a critical value, upon which a collapse of the turbulent field is predicted.

Simulations with the 1DV Point Model indeed show such a catastrophic collapse, which is caused by a positive feedback between the suspended sediment and the turbulence field when the flow velocity is (slightly) decreased or the sediment load is (slightly) increased. These numerical simulations sustain the scaling law for saturation, derived from an analysis of the behavior of stratified fluids. With this scaling law the suspended sediment concentrations, observed in the Yellow River, can be predicted to the right order of magnitude.

The analyses predict a collapse of the turbulence field at already very low concentrations (24 mg/L for a flow of 0.2 m/s at a water depth of 16 m). Whether such a collapse will occur

in nature depends upon whether or not a fluid mud layer will be formed. Such a fluid mud layer can be formed if the timescale for deposition is larger than the timescale for consolidation: At the surface of rapid consolidating layers, turbulence production is possible, and no collapse will occur. Moreover, even if a fluid mud layer would survive consolidation for the 24 mg/L case, its thickness would be <1 cm and will therefore probably not exceed the height of common bed irregularities. At these irregularities, turbulence production is possible, and a collapse of turbulence is not likely. This implies that from a practical point of view, the theory presented in this paper is applicable to higher concentrations only, when fluid mud layers of at least several centimeters (maybe even a few decimeters) thick can be formed [see also *Winterwerp*, 2001b].

This study is carried out for conditions at constant flow rate. This is typical for rivers, estuaries, and confined occurrences of high-concentrated mud suspensions in the coastal zone. The behavior described in the present paper has also been observed in simulations of high-concentrated suspensions in open sea with a full three-dimensional model, which includes the feedback between suspended sediment concentration, bed friction, and energy slope.

In the case of a constant energy slope in a 1DV model, a different behavior is to be expected. As turbulence dampens, because of sediment-induced stratification effects, the effective bed friction will decrease and the flow will accelerate. During acceleration, more turbulence is produced, which may distort the stratification effects. As a result, nonunique solutions may occur: Low current velocity and a high bed friction may yield the same energy slope as a high current velocity and low bed friction. These conditions have, however, not been addressed in the present paper.

It is interesting to note that multiplication of c_s from (3) with u and integration over the water depth h yields a transport formula for saturated suspensions:

$$F_s = \int_h c_s u \, dz \propto \tau_b u_* U/\Delta g W_s,$$

which is almost identical to the transport formula by *Bagnold* [1966] for suspended sand transport:

$$F_{\text{Bag}} = \frac{e_s(1 - e_b)\tau_b U^2}{(\rho_s - \rho_w) g W_s}. \tag{14}$$

The latter was obtained from energy considerations for uniform, steady flow in open channels with an unlimited amount of sediment on the bed. In analogy to Bagnold's transport formula the sediment transport capacity of the flow F_s can be regarded as a transport formula for saturated suspensions. Gradients in F_s would indicate whether the flow can absorb more sediment or whether supersaturated conditions may occur.

The saturation concept and the numerical simulations also shed some new light on the generation and behavior of mud banks in coastal areas. The layers of fluid mud encountered in these areas seem to be the result of autosaturation processes: Waves mobilize more sediment than can be kept in suspension.

The literature and the analyses presented in the present paper leave no doubt on the occurrence of sediment-induced buoyancy effects at already moderate hydrosedimentological conditions, resulting in an appreciable interaction between the suspended sediment and the turbulent flow field. The present analysis predicts that this interaction can result in a catastrophic behavior of suspensions of cohesive sediment, resulting in a total collapse of the vertical concentration and turbulence profile. This is very similar to the behavior of submarine turbidity currents: If too little turbulent energy is available to keep all the sediment in suspension, the turbulence will die, the sediment will settle and, as a consequence, the turbidity current itself will die [e.g., *Parker et al.*, 1986].

This saturation behavior is plausible from a physical point of view, as also suggested by *Wolanski et al.* [1992]. Though it is indirectly supported by field observations, it is stressed that at present no definite empirical proof of such catastrophic behavior exists. It is recommended that such proof is gained, either through dedicated field surveys, or laboratory experiments, prior to further theoretical analyses and improvement of turbulence closure schemes, or developments of numerical models.

Notation

b width of flow (flume).
C_0 initial suspended sediment concentration, homogeneous over water depth.
C_s depth-averaged saturation concentration.
c suspended sediment concentration by mass.
c_{gel} gelling concentration.
c_s local saturation concentration.
$c_{1\varepsilon}$ coefficient in k-ε turbulence model.
$c_{2\varepsilon}$ coefficient in k-ε turbulence model.
$c_{3\varepsilon}$ coefficient in k-ε turbulence model.
c_μ coefficient in k-ε turbulence model.
D particle size.
g acceleration of gravity.
h water depth.
h_s sedimentation depth.
K_s coefficient in scaling law for saturation.
k turbulent kinetic energy.
k_s Nikuradse's roughness height.
p pressure.
Ri_f flux Richardson number.
$Ri_{f,cr}$ critical flux Richardson number.
S salinity.
T_{rel} relaxation time.
t time.
U depth-averaged horizontal flow velocity.
u horizontal flow velocity.
u_* shear velocity.
W_s constant or characteristic settling velocity.
w vertical velocity.
w_s effective settling velocity.
x coordinate in longitudinal direction.
Z_b bed level.
Z_s level of water surface.
z vertical co-ordinate.
zb_c roughness height for waves and current.
z_0 roughness height.
β Rouse parameter.
β exponent in hindered settling formula.
Γ_c diffusion coefficient in consolidation formula.
Γ_T eddy diffusivity.
Δ relative sediment density, $\Delta \equiv (\rho_s - \rho_w)/\rho_w$.
Δt time step in 1DV point model.
Δz grid size in 1DV point model.

ε turbulent energy dissipation.
ζ relative height above bed, equal to z/h.
κ Von Kármàn constant.
κ_s effective Von Kármàn constant.
λ friction coefficient.
ν kinematic viscosity.
ν_T eddy viscosity.
ρ bulk density of water-sediment suspension.
ρ_{ref} reference concentration, equal to ρ_s or c_{gel}.
ρ_s density of primary sediment particles.
ρ_w density of water.
σ_T Prandtl-Schmidt number relating eddy diffusivity and eddy viscosity.
τ_b bed shear stress.
τ_c flow-induced bed shear stress.
τ_s surface shear stress.
τ_{sf} side wall friction.
ϕ volumetric concentration of mud flocs.

Subscripts

ξ_0 initial conditions.
ξ_s saturation conditions.

Superscripts and Other Symbols

ξ' turbulent fluctuating part of ξ.
$\bar{\xi}$ mean value of ξ averaged over turbulent timescale.

Acknowledgments. This work was partially funded by the European Commission, Directorate General XII for Science, Research and Development through the COSINUS project within the framework of the MAST-3 programme, contract MASC3-CT97-0082, by Rijkswaterstaat, Netherlands Ministry of Transport and Public works through their SILTMAN project, and by corporate research funds from Delft Hydraulics. The valuable advice from and fruitful discussions with C. Kranenburg of Delft University of Technology and R. E. Uittenbogaard from Delft Hydraulics are gratefully acknowledged. J. M. Cornelisse helped with the implementation of the various equations in the 1DV Point Model and R. Bruinsma with many graphs, both from Delft Hydraulics. I like to thank J. A. Battjes of Delft University of Technology for his comments and encouragement.

References

Adams, C. E., and G. L. Weatherly, Some effects of suspended sediment stratification on an oceanic bottom boundary layer, *J. Geophys. Res.*, *86*(C5), 4161–4172, 1981.

Adams, C. E., J. T. Wells, and Y.-A. Park, Internal hydraulics of a sediment-stratified channel flow, *Mar. Geol.*, *95*, 131–145, 1990.

Bagnold, R. A., An approach to the sediment transport problem from general physics, in *Physiographic and Hydraulic Studies of Rivers*, *U.S. Geol. Surv. Prof. Pap.*, *422*-I, 1966.

Barenblatt, G. F., On the motion of suspended particles in a turbulent stream, *Prikladnaja Mat. Mekh.*, Engl. Trans., *17*, 261–274, 1953.

Brush, L. M., M. G. Wolman, and B.-W. Huang, Taming the Yellow River: Silt and floods, in *Proceedings of a Bilateral Seminar on Problems in the Lower Reaches of the Yellow River, China*, pp. 148–165, Kluwer Acad., Norwell, Mass., 1989.

Burchard, H., and H. Baumert, On the performance of a mixed-layer model on the k-ε turbulence closure, *J. Geophys. Res.*, *100*(C5), 8523–8540, 1995.

Cellino, M., and W. H. Graf, Sediment-laden flow in open channels under non-capacity and capacity conditions, *J. Hydraul. Eng.*, *125*(5), 456–462, 1999.

Coleman, N. L., Velocity profiles with suspended sediment, *J. Hydraul. Res.*, *19*(3), 211–229, 1981.

Coleman, N. L., Reply, *J. Hydraul. Res.*, *22*(4), 275–289, 1984.

Coleman, N. L., Effects of suspended sediment on the open-channel velocity distribution, *Water Resour. Res.*, *22*(10), 1377–1384, 1986.

de Wit, P. J., Liquefaction of cohesive sediments caused by waves, Ph.D. thesis, Fac. of Civ. Eng., Delft Univ. of Technol., Delft, Netherlands, 1995.

Einstein, H. A., and N. Chien, Effects of heavy sediment concentration near the bed on velocity and sediment distribution, *MRD Sediment Ser. 8*, Univ. of Calif., Berkeley, 1955.

Elata, E., and A. T. Ippen, The dynamics of open channel flow with suspensions of neutrally buoyant particles, *Tech. Rep. 45*, Hydrodyn. Lab., Mass. Inst. of Technol., Cambridge, 1961.

Ellison, T. H., Turbulent transport of heat and momentum from an infinite rough plate, *J. Fluid Mech.*, *2*, 456–466, 1957.

Fukushima, Y., and M. Fukuda, Analysis of turbulent structure of open-channel flow with suspended sediment, *J. Hydrosci. Hydraul. Eng.*, *4*(2), 47–54, 1986.

Galland, J.-C., Transport de sédiments en suspension et turbulence, *Rapp. HE-42/96/007/A*, Electr. de Fr., Dir. des Etudes et Rech., Paris, 1996.

Galland, J.-C., D. Laurence, and C. Teisson, Simulating turbulent vertical exchange of mud with a Reynolds stress model, in *Proceedings of the 4th Nearshore and Estuarine Cohesive Sediment Transport Conference INTERCOH'94, July 1994, Wallingford, UK*, edited by T. N. Burt, W. R. Parker, and J. Watts, pp. 439–448, John Wiley, New York, 1997.

Gelfenbaum, G., and J. D. Smith, Experimental evaluation of a generalized suspended-sediment transport theory, in *Shelf Sands and Sandstones*, edited by R. J. Knight and J. R. McLean, pp. 133–144, Can. Soc. of Pet. Eng., Calgary, Alberta, 1986.

Grant, W. D., and O. S. Madsen, Combined wave and current interaction with a rough bottom, *J. Geophys. Res.*, *84*(C4), 1797–1808, 1979.

Gust, G., Discussion of N. L. Coleman's "Velocity profiles with suspended sediment," *J. Hydraul. Res.*, *22*(4), 263–275, 1984.

Hino, M., Turbulent flow with suspended particles, *J. Hydraul. Div. Am. Soc. Civ. Eng.*, *89*(HY4), 161–185, 1963.

Hopfinger, E. J., Turbulence in stratified fluids: A review, *J. Geophys. Res.*, *92*(C5), 5287–5303, 1987.

Itakura, T., and T. Kishi, Open channel flow with suspended sediments, *J. Hydraul. Div. Am. Soc Civ. Eng.*, *106*(HY8), 1325–1343, 1980.

Kachel, N. B., and J. D. Smith, Sediment transport nd deposition on the Washington continental shelf, in *Coastal Oceanography of Washington and Oregon*, *Elsevier Oceanogr. Ser.*, vol. 47, edited by M. R. Landry and B. M. Hickey, pp. 287–348, Elsevier Sci., New York, 1989.

Kineke, G. C., Fluid muds on the Amazon continental shelf, Ph.D. thesis, Univ. of Wash., Seattle, 1993.

Kineke, G. C., and R. W. Sternberg, Distribution of fluid muds on the Amazon continental shelf, *Mar. Geol.*, *125*, 193–233, 1995.

Kineke, G. C., R. W. Sternberg, J. H. Trowbridge, and W. R. Geyer, Fluid mud processes on the Amazon continental shelf, *Cont. Shelf Res.*, *16*(5/6), 667–696, 1996.

Kranenburg, C., Saturation concentration of suspended fine sediment—Computations with the Prandtl mixing-length model, *Rep. 5-98*, Fac. of Civ. Eng. and Geosci., Delft Univ. of Technol., Delft, Netherlands, 1998.

Lau, Y. L., and V. H. Chu, Suspended sediment effect on turbulent diffusion, paper presented at 22nd IAHR Congress, Lausanne, France, 1987.

Lienhard, J. H., and C. W. Van Atta, The decay of turbulence in thermally stratified flow, *J. Fluid Mech.*, *210*, 57–112, 1990.

Lyn, D. A., Turbulence and turbulent transport in sediment-laden open-channel flows, *Rep. KH-R-49*, W. M. Keck Lab. of Hydraul. and Water Resour., Div. of Eng. and Appl. Sci., Calif. Inst. of Technol., Pasadena, 1986.

Lyn, D. A., A similarity approach to turbulent sediment-laden flows in open channels, *J. Fluid Mech.*, *193*, 1–26, 1988.

Malcherek, A., Mathematische Modellierung von Strömungen und Stofftransportprozessen in Ästuaren, dissertation, Inst. für Strömungsmech. und Elektron. Rechnen im Bauwesen der Univ. Hannover, Hannover, Germany, 1995.

Muste, M., and V. C. Patel, Velocity profiles for particles and liquid in open-channel flow with suspended sediment, *J. Hydraul. Eng.*, *123*(9), 742–751, 1997.

Nezu, I., and H. Nakagawa, *Turbulence in Open-Channel Flows*, A. A. Balkema, Brookfield, Vt., 1993.

Qi, P., Y. Zhao, and Z. Y. Fan, Analyses on transport and evolution of high concentration flood in lower reaches of the Yellow River in

1977 (in Chinese), in *Movement Laws and Application Prospects of Hyper-concentrated Flow in Yellow River*, edited by P. Qi, W. L. Zhao, and M. Q. Yang, pp. 75–91, Yellow River Comm., New China Publ., Beijing, 1993.

Parker, G., Y. Fukushima, and H. M. Pantin, Self-accelerating turbidity currents, *J. Fluid Mech.*, *171*, 145–181, 1986.

Rodi, W., *Turbulence Models and Their Applications in Hydraulics—A State-of-the-Art Review*, A. A. Balkema, Brookfield, Vt., 1984.

Soulsby, R. L., and B. L. S. A. Wainwright, A criterion for the effect of suspended sediment on near-bottom velocity profiles, *J. Hydraul. Res.*, *25*(3), 341–356, 1987.

Soulsby, R. L., L. Hamm, G. Klopman, D. Myrhaug, R. R. Simons, and G. P. Thomas, Wave-current interaction within and outside the bottom boundary layer, *Coastal Eng.*, *21*, 41–69, 1993.

Taylor, P. A., and K. R. Dyer, Theoretical models of flow near the bed and their implications for sediment transport, in *The Sea*, vol. 6, *Marine Modeling*, edited by E. D. Goldberg et al., pp. 579–601, John Wiley, New York, 1977.

Teisson, C., O. Simonin, J.-C. Galland, and D. Laurence, Turbulence modelling and mud sedimentation: A Reynolds stress model and a two-phase flow model, paper presented at the 23rd International Conference on Coastal Engineering, Venice, Italy, Oct. 1992.

Tennekes, H., and J. L. Lumley, *A First Course in Turbulence*, MIT Press, Cambridge, Mass., 1994.

Trowbridge, J. H., and G. C. Kineke, Structure and dynamics of fluid muds on the Amazon continental shelf, *J. Geophys. Res.*, *99*(C1), 865–874, 1994.

Turner, J. S., *Buoyancy Effects in Fluids*, Cambridge Univ. Press, New York, 1973.

Uittenbogaard, R. E., Physics of turbulence: technical report on subtask 5.2, *Rep. Z649*, MAST VERIPARSE Project, Delft Hydraul., Delft, Netherlands, 1994.

Uittenbogaard, R. E., The importance of internal waves for mixing in a stratified estuarine tidal flow, Ph.D. thesis, Delft Univ. of Technol., Delft, Netherlands, Sept. 1995a.

Uittenbogaard, R. E., Observations and analysis of random internal waves and the state of turbulence, paper presented at IUTAM Symposium on Physical Limnology, Int. Union of Theoret. and Appl. Mech., Broome, Western Australia, Sept. 10–14, 1995b.

Valiani, A., An open question regarding shear flow with suspended sediments, *Meccanica*, *23*, 36–43, 1988.

van der Ham, R., Turbulent exchange of fine sediments in tidal flow, Ph.D. thesis, Fac. of Civ. Eng. and Geotech. Sci., Delft Univ. of Technol., Delft, Netherlands, 1999.

van der Ham, R., C. Kranenburg, and J. C. Winterwerp, Turbulent vertical exchange of fine sediments in stratified tidal flows, in *Proceedings of the Conference on Physical Processes in Estuaries and Coastal Seas (PECS)*, edited by J. Dronkers and M. B. A. M. Scheffers, pp. 201–208, A. A. Balkema, Brookfield, Va., 1998.

van Kessel, T., Generation and transport of subaqueous fluid mud layers, Ph.D. thesis, Dep. of Civ. Eng., Delft Univ. of Technol., Delft, Netherlands, 1997.

Van Kesteren, W. G. M., J. M. Cornelisse, and C. Kuijper, DYNASTAR bed model: Bed strength, liquefaction and erosion, *Series on Cohesive Sediments, Rep. 55*, Rijkswaterstaat and WL Delft Hydraul., Delft, Netherlands, 1997.

Vanoni, V. A., Transportation of suspended sediment by water, *ASCE Trans.*, *111*, 67–133, 1946.

Vanoni, V. A., and G. N. Nomicos, Resistance properties of sediment-laden streams, *Trans. ASCE*, *125*, 1140–1175, 1960.

van Rijn, L. C., Mathematical modelling of morphological processes in the case of suspended sediment transport, Ph.D. thesis, Fac. of Civ. Eng., Delft Univ. of Technol., Delft, Netherlands, 1987.

Wan, Z. H., and Z. Y. Wang, *Hyperconcentrated Flow*, A. A. Balkema, Brookfield, Vt., 1994.

West, J. R., and K. O. K. Oduyemi, Turbulence measurements of suspended solids concentration in estuaries, *J. Hydraul. Eng.*, *115*(4), 457–474, 1989.

Wiberg, P. L., D. E. Drake, and D. A. Cacchione, Sediment resuspension and bed armoring during high bottom stress events on the northern California inner continental shelf: Measurements and predictions, *Cont. Shelf Res.*, *14*(10/11), 1191–1219, 1994.

Winterwerp, J. C., On the dynamics of high-concentrated mud suspensions, Ph.D. thesis, Delft Univ. of Technol., Delft, Netherlands, 1999.

Winterwerp, J. C., Flocculation and fluid mud formation, *Cont. Shelf Res.*, in press, 2001a.

Winterwerp, J. C., Scaling parameters for saturated mud suspensions, paper presented at the 6th Nearshore and Estuarine Cohesive Sediment Transport Conference INTERCOH-2000, Delft, Netherlands, 2001b.

Winterwerp, J. C., R. E. Uittenbogaard, and J. M. de Kok, Rapid siltation from saturated mud suspensions, in *Coastal and Estuarine Fine Sediment Processes, Elsevier Proc. Mar. Sci.*, vol. 3, edited by W. H. McAnally and A. J. Mehta, pp. 125–146, Elsevier Sci., New York, 2001.

Wolanski, E., J. Chapell, P. Ridd, and R. Vertessy, Fluidization of mud in estuaries, *J. Geophys. Res.*, *93*(C3), 2351–2361, 1988.

Wolanski, E., R. J. Gibbs, Y. Mazda, A. J. Mehta, and B. King, The role of turbulence in settling of mudflocs, *J. Coastal Res.*, *8*(1), 35–46, 1992.

Wright, L. D., S.-C. Kim, and C. T. Friedrichs, Across-shelf variations in bed roughness, bed stress and sediment suspension on the northern California shelf, *Mar. Geol.*, *154*, 99–115, 1999.

Zhou, D., and J. R. Ni, Effects of dynamic interaction on sediment-laden turbulent flows, *J. Geophys. Res.*, *100*(C1), 981–996, 1995.

J. C. Winterwerp, Faculty of Civil Engineering and Geosciences, Delft University of Technology, P.O. Box 5048, 2600 GA Delft, Netherlands. (h.winterwerp@ct.tudelft.nl)

(Received May 15, 2000; revised February 9, 2001;
accepted February 26, 2001.)